Agricultural Water Management 141 (2014) 10–22

Contents lists available at ScienceDirect

Agricultural Water Management

journal homepage: www.elsevier.com/locate/agwat

# Evaluation of soil water dynamics and crop yield under furrow irrigation with a two-dimensional flow and crop growth coupled model

Jun Wang[a,b], Guanhua Huang[a,b,*], Hongbin Zhan[c], Binayak P. Mohanty[d], Jianhua Zheng[a,b], Quanzhong Huang[a,b], Xu Xu[a,b]

[a] Center for Agricultural Water Research, China Agricultural University, Beijing 100083, China
[b] Chinese-Israeli International Center for Research and Training in Agriculture, China Agricultural University, Beijing 100083, China
[c] Department of Geology and Geophysics, Texas A&M University, College Station, TX, USA
[d] Department of Biological and Agricultural Engineering, Texas A&M University, College Station, TX, USA

ARTICLE INFO

*Article history:*
Received 18 January 2013
Received in revised form
26 December 2013
Accepted 5 April 2014

*Keywords:*
HYDRUS
Coupled model
Drip irrigation
Crop growth model
Root water uptake

ABSTRACT

Aiming at investigating an appropriate furrow irrigation management strategy for high melon yields and water productivity (WP), a new coupled model was developed based on the CHAIN_2D and the crop growth model of EPIC. In the coupled model, the root water uptake model of Vrugt was coupled with the root depth growth model in order to consider the interaction between root water uptake and crop growth. The coupled model was calibrated and validated with the observed values obtained from melon field experiment conducted in 2008 and 2009 in Gansu province, Northwest China. Simulation of total water use, leaf area index, melon yield and soil water dynamics fitted well with the field observations. The calibrated model was then used to predict the yield and water productivity (WP) of melon under different furrow irrigation scenarios. The relative yield and WP for different irrigation depth were considered as the criteria for investigating the appropriate irrigation management practices. Results showed that the relative yield and WP increased and decreased, respectively, as the relative irrigation increased through a quadratic function. The appropriate irrigation amounts for melon in the study area were 209 mm and 218 mm in 2008 and 2009, respectively.



## 1. Introduction

Water shortage is of great concern for crop production in the arid areas of northwest China (Kang et al., 2004). Melon is one of the main horticultural and cash crops in the oasis arid region of Shiyang River basin, Gansu Province, Northwest China. Furrow irrigation is one of the main irrigation methods for melon. Irrigation quota for melon is about 4050 $m^3$ $ha^{-1}$. Many studies indicated that the water use efficiency (WUE) in this area was very low (Kang et al., 1996) because of relatively high irrigation rates used by local farmers. Wöhling and Schmitz (2007) indicated that optimal water application control in irrigated agriculture had a high potential for increasing WUE and for creating sustainable irrigation system. However, field experiments are time-consuming and expensive. Therefore, process-based simulation tools with crop growth are required for evaluating and predicting crop yield and water requirement under furrow irrigation.

For furrow irrigation, a two-dimensional model should be used for soil water dynamics. Many models have been developed to simulate water flow in two-dimensional (2D) transport domain including SWMS_2D (Šimůnek et al., 2008), CHAIN_2D (Šimůnek et al., 2008), Nitrogen-2D (Lu et al., 2004). Among them, HYDRUS-2D (Šimůnek et al., 2008) is the most widely used model to simulate two dimensional movements of water, heat, and solute in variably saturated media. Recent studies have shown that HYDRUS-2D can be used to quantitatively evaluate deep percolation and nitrogen leaching under furrow irrigation with complex boundary conditions in the absence and presence of plants (Hanson et al., 2006; Doltra and Muñoz, 2010; Mmolawa and Or, 2003). Mailhol et al. (2007) applied HYDRUS-2D to evaluate the impact of water application condition on nitrogen leaching under furrow irrigation. Crevoisier et al. (2008) used HYDRUS-2D to simulate water and nitrogen transfer under two furrow irrigation technologies—every

* Corresponding author at: China Agricultural University, Center for Agricultural Water Research, Beijing 100083, China. Tel.: +86 10 62737144; fax: +86 10 62737138.
*E-mail addresses:* junwangcau@gmail.com (J. Wang), ghuang@cau.edu.cn (G. Huang), zhanhb@yahoo.com (H. Zhan), bmohanty@tamu.edu (B.P. Mohanty).

http://dx.doi.org/10.1016/j.agwat.2014.04.007
0378-3774/

furrow irrigation and alternative furrow irrigation. Ajdary et al. (2007) modeled nitrogen leaching from experimental onion field under drip fertilization by HYDRUS-2D. However, the interaction of crop growth and soil water dynamics was not considered in those above models. This may has significant effects on model accuracy, especially when applying it in arid irrigated areas. Thus, integration of the soil water model and crop model is crucial to describe the soil water dynamics and crop growth under furrow irrigation in this study area. The efforts on the integration had been reported in previous references. For example, Wöhling and Schmitz (2007) developed physically based coupled model for simulating 1D surface–2D subsurface flow and plant water uptake in irrigation furrow. In this model, crop growth was considered to simulate crop yield and actual evapotranspiration. However, a simple exponential function with uniform root density distribution was applied to describe the root water uptake, which cannot describe the root growth in the horizontal direction. de Willigen et al. (2002) indicated that root distribution pattern should be known *a priori* to estimate the 2D root water uptake potential. Vrugt et al. (2001) developed a 2D distribution function of root water uptake which allows spatial variations of water uptake under non-uniform and uniform water application patterns. This root water uptake distribution model has been successfully applied in HYDRUS model (Šimůnek et al., 2008) and APRI (Zhou et al., 2007). However, the above-mentioned 2D root distribution model does not consider root growth. Furthermore, Vrugt et al. (2001) indicated that the root water uptake distribution model can be adapted to account for root growth by allowing time-dependent $Z_m$ and $X_m$ values during a growing season. Therefore, it is necessary to develop a 2D framework with a simplified crop growth model and root water uptake distribution model considering root growth to simulate the soil water transport, root water uptake and crop yield in the vadose zone especially for an annual crop such as melon, which is the primary objective of this study.

Simplified models with easily measurable inputs were preferred at field production level (Wang and Smith, 2004). With less-demanding data input, the crop growth model of EPIC uses a unified approach to simulate the growth for more than 80 types of crops (Williams et al., 2006). Therefore, in this study, crop growth was simulated using a simplification of the EPIC crop growth model (Williams et al., 1989) including crop phonological development based on daily accumulated heat unit, a harvest index for partitioning grain yield, Monteith's approach (Monteith, 1977) for potential biomass, and water and temperature stress adjustments. Li et al. (2007) used the crop growth model of EPIC to develop the water and nitrogen management model (WNMM) for intensive cropping systems.

The objectives of this study are (a) to develop a model based on CHAIN_2D coupled with crop growth model of EPIC to simulate the dynamic root growth, root water uptake and crop yield under furrow irrigation, (b) to calibrate and validate the coupled model using melon field experimental data, and (c) to use the coupled model to estimate the yield and water productivity (WP) under different furrow irrigation scenarios for melon in the study area and subsequently obtain appropriate irrigation amounts for the study period.

## 2. Materials and methods

### 2.1. Field experiment

#### 2.1.1. Experimental site

For the purpose of testing the proposed coupled model that will be described in detail later, we conducted experiments in the melon growing seasons of 2008 and 2009 at the Shiyanghe Experimental Station of China Agricultural University, located in Wuwei city, Gansu province, China (102°50′E, 37°52′N, altitude 1581 m). The experimental site is in a typical continental temperate climate zone, with a mean annual temperature of 8 °C, an average annual sunshine duration of 3000 h, a mean annual precipitation of 164 mm, a mean annual pan evaporation rate of about 2000 mm. The groundwater table is 40–50 m below the ground surface (Li et al., 2008).

Soils in the experimental site are sandy loam at the depth of 0–30 cm and silt loam at depths larger than 30 cm. The bulk density is in the range of 1.44–1.58 g $cm^{-3}$, field capacity ranges from 0.24 to 0.34 $cm^3$ $cm^{-3}$, and the wilting point ranges from 0.06 to 0.12 $cm^3$ $cm^{-3}$. The soil physical properties of the experimental site are presented in Table 1.

#### 2.1.2. Experimental design

Huanghemi No. 3 (*Cucumis melo L.*), a widely growing melon species was used in the field trial. The sowing and harvesting dates were May 8th and August 25th, respectively. The emergence day of melon was May 17th. Irrigation water was applied to the field based on the lower soil water content (SWC) limit in the root zone. Each lower SWC limit corresponds to a percentage of field capacity (FC). The top 0–50 cm of soil layer was considered as the main root zone of melon in the following analysis according to Sensoy et al. (2007). Refilling to field capacity was performed as the average SWC in the root zone approached the proposed lower SWC limits for irrigation. There were two treatments, i.e. T1 and T2 which were applied in 2008 and 2009, respectively. The lower SWC limit for irrigation of T1 and T2 was 55% and 65% FC during blooming to swelling stages, respectively. The lower SWC limit during seedling and mature stages were 55% FC for T1 and T2. According to the results of the literature (Li et al., 2012), both treatments T1 and T2 can be considered as a moderately water stress treatment and a slightly water stress treatment, respectively. Each treatment had three replicates. The irrigation depth and timing of the T1 and T2 are shown in Table 2. Water was provided to the furrows by using a 20 mm diameter hose with an attached flow meter to record the applied water. The size of each subplot was 43.2 $m^2$ (8 m × 5.4 m), comprised of 6 rows with 17 plants per row. The spacing between rows and plants was 1.0 m and 0.5 m, respectively. The size of furrow and row is shown in Fig. 1. The furrow length is 8 m, and slop of the furrow is about 0.001. The furrow was partially covered by white plastic, a practice widely used in this area for many years. It covered 0.5 m of the soil and was placed on the row before melon seeding (Fig. 1). Besides, there was a 1-m empty gap between plots to eliminate any water disturbance from adjacent plots.

#### 2.1.3. Measurement

Solar radiation, air temperature, rainfall, wind speed and relative humidity were measured every 15 min at a weather station (Hobo Weather Station, Campbell Scientific Inc., USA) which was about 50 m away from the experiment site.

The spatial distribution of melon root was measured using an 8 cm diameter auger. Soil cores were taken from three locations of furrow cross-section at depths of 20, 40, 60, 80, 100 cm on July 22th in the plots of T2 (Fig. 1) because few roots were found below the depth of 100 cm. The maximum root elongation in the horizontal direction is about 50 cm. In addition, soil core were taken from plant point to measure the root depth on DAE (day after emergence) 26, DAE42, DAE50, DAE67 and DAE98. The dimensions of each soil core sample were 8 cm (diameter) and 10 cm (depth). There were 28 samples to measure the root length density in the cross section of the furrow. Roots were washed from the soil core samples. The root length of each sample was measured by the scanner (Regent Instruments Inc., Canada), and the root length density (cm $cm^{-3}$) was calculated by the total root length over the soil core volume.

**Table 1**
Measured soil physical properties at the experiment site.

| Soil depth (cm) | Sand (%) | Silt (%) | Clay (%) | Soil texture | Bulk density ($g\,cm^{-3}$) | Field capacity ($cm^3\,cm^{-3}$) | Wilting point ($cm^3\,cm^{-3}$) |
|---|---|---|---|---|---|---|---|
| 0–10 | 49.72 | 47.29 | 2.99 | Sandy loam | 1.50 | 0.24 | 0.06 |
| 10–30 | 51.45 | 45.77 | 2.78 | Sandy loam | 1.58 | 0.25 | 0.06 |
| 30–60 | 43.52 | 53.33 | 3.15 | Silt loam | 1.51 | 0.28 | 0.08 |
| 60–90 | 18.39 | 78.02 | 3.59 | Silt loam | 1.44 | 0.34 | 0.12 |
| 90–120 | 18.73 | 75.14 | 6.13 | Silt loam | 1.47 | 0.34 | 0.11 |

**Table 2**
Irrigation amount (mm) of T1 and T2.

| Growth stage | Seedling | Blooming to fruit setting | | Fruit swelling | | | |
|---|---|---|---|---|---|---|---|
| Time | DAE 11 | DAE 33 | DAE 48 | DAE 53 | DAE 60 | DAE 71 | DAE 78 |
| T1 | 32.5 | 0.0 | 0.0 | 62.6 | 0.0 | 78.7 | 0.0 |
| T2 | 0.0 | 43.9 | 45.7 | 0.0 | 47.6 | 39.6 | 41.4 |

*Note*: DAE represents days after emergence. The irrigation amount for each furrow was determined in term of *Ir*/*F*, where *Ir* is the irrigation amount for the whole plot and *F* is the fraction of the furrow width to the width of the plot.

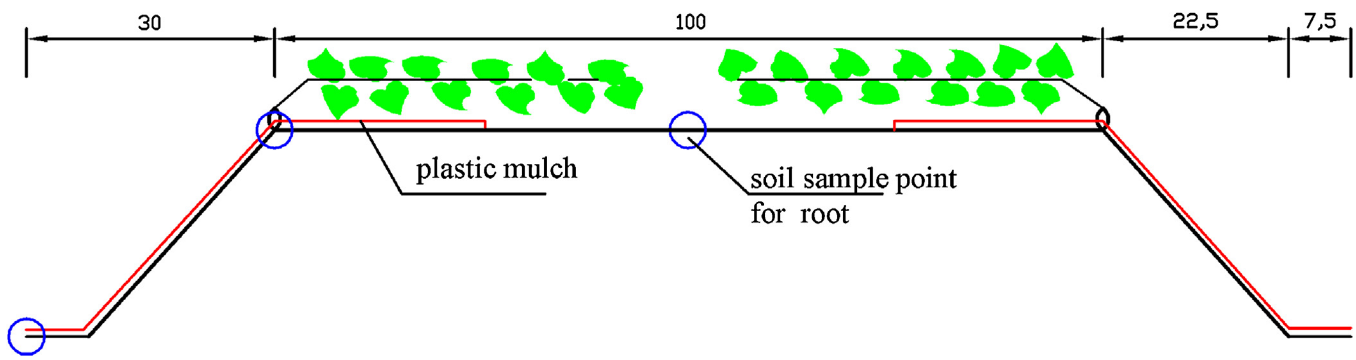


**Fig. 1.** Sketch of the furrow size.

A Time Domain Reflectometry (TDR) probe (TDR100, Compbell Scientific, Inc., USA) was used to monitor soil volumetric water content in one replicate plot of T2 treatment in 2009 season. The TDR system includes 32 three-rods-probes with a rod length of 15 cm. The sensors were installed horizontally at depths of 10, 30, 60 and 90 cm under furrow ridge and furrow side. The distribution of measurement sensors is showed in Fig. 2. Signals for soil water content were recorded every 30 min and stored in a CR3000 data logger (Campbell Scientific, Inc., USA). In addition, soil samples for soil moisture were collected every 15 days using the auger under two points corresponding to the distribution of the soil water content measurement sensors (Fig. 2) at depths of 10, 30, 60, 90 cm in 2008 and 2009. Precautions were taken to ensure that the infiltration tests were not disturbed (careful refilling of the holes where soil samples were collected). The gravimetric sampling data was used to calibrate the TDR100 display unit.

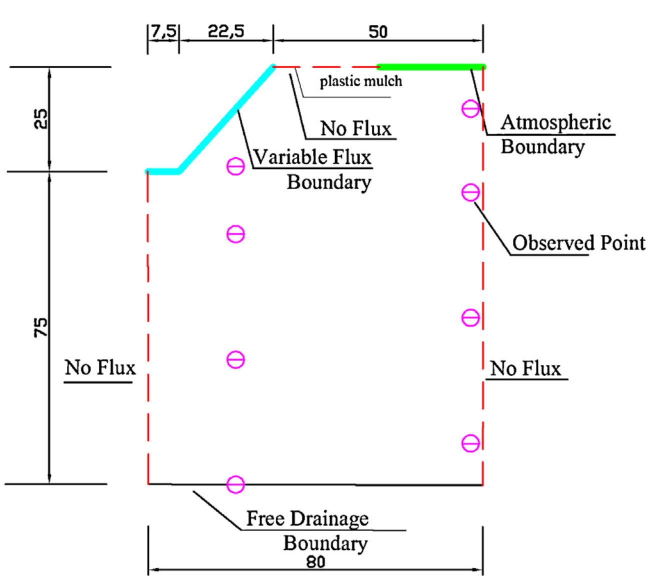


**Fig. 2.** Boundary conditions used in the coupled model.

Leaf area index (*LAI*) was measured every 15 days by the Canopy Analysis System (SunScan, Dynamax, Inc., USA) and the leaf samples were also collected in 1 $m^2$ to calibrate the SUNSCAN data. At harvest, all of the fruits in each plot were taken and weighted to determine fruit yield.

### 2.2. Model description

#### 2.2.1. Governing equation

The governing equation of flow is given by the following modified Richards' equation (Šimůnek and van Genuchten, 1994):

$$\frac{\partial \theta}{\partial t} = \frac{\partial}{\partial x_i}\left[K\left(K_{ij}^A \frac{\partial h}{\partial x_j} + K_{iz}^A\right)\right] - S, \tag{1}$$

where $\theta$ is the soil volumetric water content ($cm^3\,cm^{-3}$), $h$ is the pressure head (cm), $S$ is a sink term ($cm^3\,cm^{-3}\,d^{-1}$), representing the volume of water removed per unit time from a unit volume of soil due to root water uptake, $x_i$, $x_j$ are the spatial coordinates ($i$, $j$ = 1,2) (cm), $t$ is time (d), $K_{ij}^A$ are components of a dimensionless anisotropy tensor $K^A$, and $K$ is the unsaturated hydraulic conductivity ($\mathrm{cm\,d^{-1}}$). In this study, we assume that the porous medium is isotropic; the saturated hydraulic conductivity tensor has off-diagonal entries equal to 0 and the diagonal terms equal to the saturated hydraulic conductivity, $K_s$ ($\mathrm{cm\,d^{-1}}$). The unsaturated hydraulic conductivity $K(h)$ is determined by using the van Genuchten–Mualem (VGM) model (Mualem, 1976; van Genuchten, 1980),

$$K(h) = K_s S_e^{0.5}\left[1-\left(1-S_e^{1/m}\right)^m\right]^2, \tag{2}$$

$$S_e = \frac{\theta-\theta_r}{\theta_s-\theta_r} = \left[1+(\alpha h)^n\right]^{-m}, \quad m = 1-\frac{1}{n}, \tag{3}$$

where $S_e$ is the effective water saturation, $\theta_s$ and $\theta_r$ are the saturated and residual water contents ($\mathrm{cm^3\,cm^{-3}}$), respectively, $\alpha$, $n$, $m$ are the empirical parameters. The actual root water uptake rate $S$ can be calculated from (Šimůnek and van Genuchten, 1994)

$$S(h,x,z) = a_r(h,x,z)b(x,z)L_t T_P, \tag{4}$$

where the water stress response function $a_r(h, x, z)$ is a prescribed dimensionless function of the soil water pressure head which can be obtained from the Feddes model (Feddes et al., 1978), $b(x, z)$ is the normalized water uptake distribution ($\mathrm{cm^{-2}}$), $L_t$ is the width of soil surface associated with the transpiration process (cm), $T_p$ is the potential transpiration rate ($\mathrm{cm\,d^{-1}}$) which can be expressed as (Wöhling and Schmitz, 2007):

$$T_p = (1-\exp(-0.7LAI))K_{c,\max}(1-\exp(-LAI))ET_O, \tag{5}$$

where $ET_o$ is the reference evapotranspiration which can be calculated by the Penman–Monteith equation (Allen et al., 1998). *LAI* (leaf area index) is estimated according to Williams et al. (1989). $K_{c,max}$ is maximum possible value of crop coefficient. Potential evaporation ($E_p$) is calculated according to Wöhling and Schmitz (2007):

$$E_p = ET_O\exp(-0.7LAI), \tag{6}$$

Therefore, the actual transpiration rate $T_a$ ($\mathrm{cm\,d^{-1}}$) can be computed as follows (Šimůnek and van Genuchten, 1994):

$$T_a = T_p\int_\Omega a_r(h,x,z)\,b(x,z)\,\mathrm{d}\Omega, \tag{7}$$

where $b(x, z)$ is estimated as (Šimůnek and van Genuchten, 1994)

$$b(x,z) = \frac{b'(x,z)}{\int_\Omega b'(x,z)\mathrm{d}\Omega}, \quad \int_\Omega b(x,z)\mathrm{d}\Omega = 1, \tag{8}$$

where $\Omega$ is the region occupied by the root zone and $b'(x, z)$ is an arbitrarily prescribed distribution function and can be described with a modified form of Vrugt et al. (2001) as

$$b'(x,z) = \left(1-\frac{z}{Z_m(t)}\right)\left(1-\frac{|x-x_p|}{X_m(t)}\right) \times e^{-(p_z/Z_m(t)|z^*-z|+p_x/X_m(t)|x^*-|x-x_p||)}, \tag{9}$$

where $x$, $z$ are the distances from the origin of plant in horizontal and vertical directions, respectively; $X_m(t)$ and $Z_m(t)$are the maximum rooting length and depth in horizontal and vertical directions (cm) at time $t$, respectively; $x_p$ is the planting point (cm); $p_x$, $p_z$ are empirical parameters (Vrugt et al., 2001). $x^*$ and $z^*$ are defined as follows:

$$\begin{cases} x^* = RH, & RH \le x^{\max} \\ x^* = x^{\max}, & RH > x^{\max} \end{cases}, \tag{10a}$$

$$\begin{cases} z^* = RD, & RD \le z^{\max} \\ z^* = z^{\max}, & RD > z^{\max} \end{cases}, \tag{10b}$$

where *RH* is the root length in the horizontal direction, *RD* is the root depth (cm); $x^{max}$, $z^{max}$ are the empirical parameters (cm). For most annual crops, the rooting lengths in the horizontal and vertical directions increase with time. In addition, root water uptake in the root zone is affected by root dynamic distribution and water stress, which constrained the crop growth. Therefore, the variation of root distribution over the growing period should be considered. To describe the dynamic root distribution and the interaction between the root water uptake and crop growth, $Z_m(t)$ is obtained from the crop growth model and considered as a function of time. It can be estimated as (Williams et al., 1989)

$$\begin{cases} Z_m(t) = RD_i, & RD_i \le RD_{\max} \\ Z_m(t) = RD_{\max}, & RD_i > RD_{\max} \end{cases}, \tag{11}$$

$$\begin{cases} RD_i = 2.5RD_{\max}(HUI_i) \\ RH_i = 0.5RD_i \end{cases}, \quad RD_i \le RD_{\max}, \tag{12}$$

where *HUI* is the heat unit index which is estimated according to Williams et al. (1989), and subscripts *max* and *i* denote the maximum value possible for the crop and day time, respectively. In addition, $X_m(t)$ is assumed to be a proportion of $Z_m(t)$according to Gao et al. (2010). It can be calculated as

$$\begin{cases} X_m(t) = 0.5Z_m(t), & X_m(t) \le RH_{\max} \\ X_m(t) = RH_{\max}, & X_m(t) > RH_{\max} \end{cases}, \tag{13}$$

where $RH_{max}$ is the maximum value of the root length in the horizontal direction. In this study, the $RH_{max}$ is 50 cm.

In addition, the actual crop yield can be calculated using the harvest index concept following the EPIC model procedures (Williams et al., 1989), i.e. as a function of the above-ground biomass ($\mathrm{kg\,ha^{-1}}$) and crop growth regulation factor (*REG*). In this study, we only considered the water and temperature stresses on the crop, and then *REG* was estimated as follows (Williams et al., 1989):

$$REG = \min(WS, TS), \tag{14}$$

where *WS* and *TS* are the values of water stress and temperature stress, respectively. In this study, the water stress (*WS*) and temperature stress (*TS*) is defined according to the report of Williams et al. (1989).

The coupled model is coded in program subroutines and functions integrated with CHAIN-2D and the crop model of EPIC (Fig. 3). This model was written in FORTRAN 90 for Windows system. As shown in Fig. 3, atmospheric data was used to calculate the reference evapotranspiration $ET_o$ and to estimate the potential crop yield, root depth and potential *LAI*. Then, the calculated potential *LAI* was used to calculate the potential transpiration and evaporation (Eqs. (5) and (6)) which are the initial value of the actual crop transpiration and soil evaporation. The actual transpiration was estimated according to Wöhling and Schmitz (2007):

$$T_a(i) = \int_{t=i-1}^{i}\int_{\Omega_R} q_{root}^{(node)}(t,h)\mathrm{d}\Omega\mathrm{d}t \approx \sum_{t=i-1}^{i}\left\{\sum_{node=1}^{nrn}\left[q_{root}^{(node)}(t,h)\right]\right\}\Delta t \tag{15}$$

$$q_{root}^{(node)}(t,h) = b(x,z)S(h,x,z)T_p(i) \tag{16}$$

where $q_{root}^{(node)}(t,h)$ is the nodal flux within the root domain; $\Delta t$ is the time step for CHAIN-2D computations which was executed using

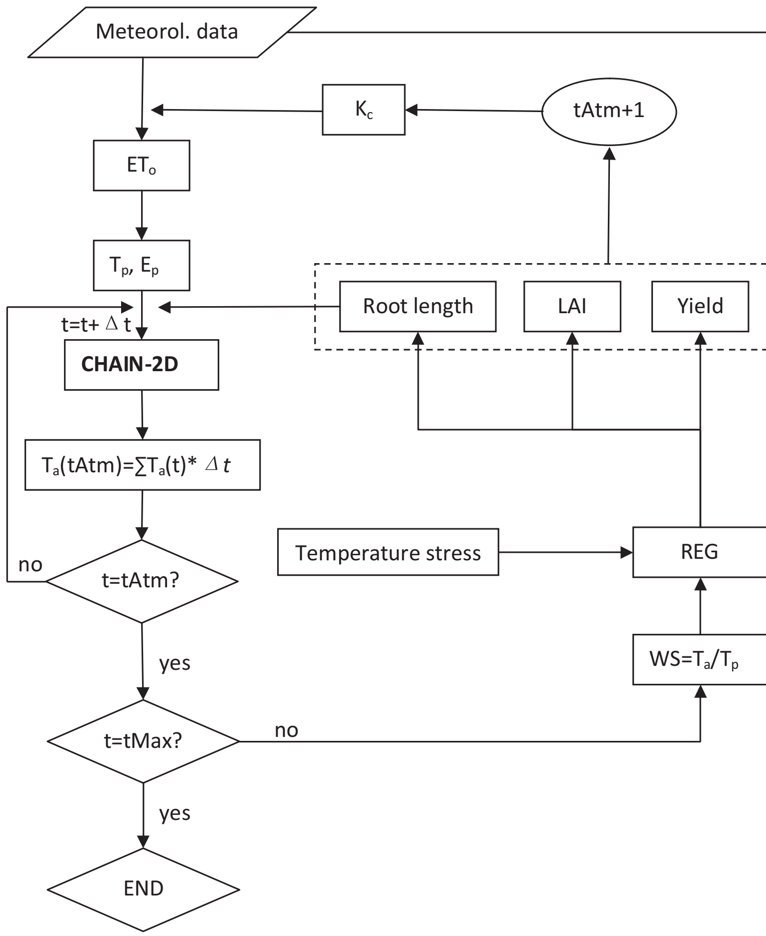


**Fig. 3.** Coupling scheme of CHAIN-2D and crop model of EPIC.

an appropriate time step $\Delta t$ to solve the Richards equation (Eq. (1)). The time step length is adapted according to the number of iterations required for solving Eq.1 (for details refer to Šimůnek and van Genuchten (1994)). $i$ is the day time, and $nrn$ is number of nodes within the root zone. This is repeated for a number of time steps until the end of the first simulation day. Then, the water stress for next day can be estimated by the actual transpiration $T_a$ in one day divided to potential transpiration $T_p$ and crop regulation factor *REG* can be obtained. Then, the output variables (i.e. actual *LAI* and yield) can be obtained.

### 2.2.2. Initial and boundary conditions

The initial condition of soil water content was based on the observation data of May 17th because the observed soil water contents were available after May 17th. Finite element mesh of numerical simulations was designed to be denser near the top boundary to avoid numerical divergence where moisture gradients are the greatest. A relatively fine grid (3 cm) was used near the soil surface and a coarser grid (5 cm) at and near the bottom of the domain. Eight observation nodes of soil water content were defined in the cross-section of subplot at the depths corresponding to the soil sampling.

The boundary condition of the simulation domain is presented in Fig. 2. It was assumed that there is no discharge of water and solute on the sides of the flow domain due to symmetry of the half-furrow and ridge. Hence, no-flux boundary condition was chosen (Mailhol et al., 2007; Ajdary et al., 2007; Abbasi et al., 2004; Siyal et al., 2012). Bottom boundary was considered as free drainage condition ascribing to the deep groundwater table (Mailhol et al., 2007; Ajdary et al., 2007; Abbasi et al., 2004). Infiltration flux and no flux in furrow covered by plastic mulch were used for irrigation and non-irrigation periods, respectively. In addition, due to the relatively small length of irrigation and infiltration last, and for the case of computation, we used a variable flux boundary instead of the variable prescribed head boundary for the furrow. The half of the ridge covered by plastic mulch was set to no-flux boundary condition since no flow crossed the surface when rainfall, irrigation and evapotranspiration occurred. The other half of the ridge was set to atmospheric boundary condition since it was not covered by plastic mulch and was open to the atmosphere. Precipitation on the variable-flux boundary was assumed as variable flux due to the fact that water can infiltrate into the soil under furrow in despite of the plastic mulching.

## 2.3. Sensitivity analysis

To investigate which parameter has the most significant effect on the yield and total water use (*TWU*), a sensitivity analysis was conducted in this study. The initial or default parameters and the observed dataset of the T2 were used as the base simulation. The input parameters included in this study are: VGM model parameters $\theta_r$, $\theta_s$, $\alpha$, $n$ *and* $K_s$, crop growth model parameters, i.e. the optimal and base temperatures $T_0$ and $T_b$, the maximum *LAI* and *RD*, harvest index *HI*, required cumulative heat unit for crop maturity *PHU* and maximum possible value of crop coefficient $K_{c,max}$. All parameters were varied by −50% to +50% with interception of 10%. In addition, the VGM parameters were changed simultaneously in all soil layers rather than independently for each layer (Wöhling and Mailhol, 2007).

**Table 3**
The range of parameters and the optimized parameters for the root distribution function.

| | $p_x$ | $p_z$ | $x^{max}$ (cm) | $z^{max}$ (cm) |
|---|---|---|---|---|
| *Min* | 0.1 | 0.1 | 0 | 0 |
| *Max* | 15 | 15 | 50 | 100 |
| Optimized | 0.3832 | 0.2307 | 0.0202 | 1.0485 |

*Note*: $p_x$, $x^{max}$, $p_z$ and $z^{max}$ are empirical parameters.

### 2.4. Calibration and validation

The measured values of soil water content and crop variables of treatments T2 and T1 were used to calibrate and validate the coupled model, respectively. The root water uptake, soil hydraulic and crop growth parameters were calibrated and validated in this study. An iterative calibration approach was adopted to account for the interactions between water flow and crop growth process. The calibration process was first performed for the root water uptake, then for water flow, finally for the crop growth and yield.

Genetic algorithm (GA) was applied to get the optimized root water uptake parameters of the Vrugt model based on the observed root length density of the soil core samples for the root. The fitness function for GA was described as follows (Vrugt et al., 2001):

$$OF(\mathbf{s}) = \frac{1}{n}\sum_{i=1}^{n}\left[b'(x,z) - b(x,z;\mathbf{s})\right]^2 \tag{17}$$

where $OF(\mathbf{s})$ is the objective function, $n$ is the number of measurements, $b'(x,z)$ and $b(x,z;\mathbf{s})$ are the measured and predicted root length density at the point $(x,z)$, respectively; $\mathbf{s}$ is the parameter vector representing the fitting parameters. For a relatively fast convergence to the global optimum, we used a relatively high crossover fracture value of 0.8 (Vrugt et al., 2001). In addition, the population size and generations was 30 and 1000, respectively. Smaller values of the objective function $OF(\mathbf{s})$ imply that better fitting is obtained. The allowable ranges of the parameters included in $\mathbf{s}$ are shown in Table 3 according to Vrugt et al. (2001). The GA optimization was carried out using MATLAB (version 7.12.0 (R2011a), the Math Work, Inc, 2011).

The initial input soil hydraulic parameters were predicted by Rosetta Lite (v.1.1) in HYDRUS with the dataset of the soil particle-size distribution and bulk density presented in Table 1. However, the soil hydraulic parameters should be calibrated ascribed to the spatial variability of the soil in the field condition. The soil water contents in different soil layers under the furrow side and middle ridge along the crop growing period for T2 and T1 treatments were used to calibrate and validate the soil hydraulic parameters, respectively. The hydrologic component was calibrated by trial and error using the measured soil water contents in different soil layers (S-10, S-30, S-60, S-90 and M-10, M-30, M-60, M-90). In addition, two different statistical indexes were used to evaluate the model performance for predicting soil water contents according to the criteria proposed by Willmott (1982). These two indices, including mean absolute error (*MAE*) and root mean square error (*RMSE*), represent the discrepancy between observations and predictions. The closer *RMSE* is to 0, the more accurate the model is. These two indices were described as follows:

$$MAE = \frac{\sum_{i=1}^{n}\left|O_i - P_i\right|}{n}, \tag{18}$$

$$RMSE = \sqrt{\frac{\sum_{i=1}^{n}(O_i - P_i)^2}{n}}, \tag{19}$$

where $O_i$ and $P_i$ are the observed and simulated values respectively, $n$ is the number of the pair values. The soil hydraulic component was considered as good calibration when the *MAE* and *RMSE* values of the simulated soil water contents were both lower than 0.03 $cm^3\,cm^{-3}$ (Crevoisier et al., 2008; Zhou et al., 2007). In addition, the Nash and Sutcliffe model efficiency (*NSE*) was also used to quantify the model performance. The *NSE* was calculated as

$$NSE = 1 - \frac{\sum_{i=1}^{n}(P_i - O_i)^2}{\sum_{i=1}^{n}\left(O_i - O_{avg}\right)^2} \tag{20}$$

where $O_{avg}$ is the mean observed value. The *NSE* values range from $-\infty$ (poor model) to unity (perfect model). A value of zero for the *NSE* means the simulated value is as good as the observed mean.

The initial parameters of crop growth were estimated from the default values of the EPIC model or published literature. In this study, the initial crop coefficients were adjusted according to the suggestion of FAO 56 (Allen et al., 1998) in which crop coefficient during the initial, middle and end of the growth period was 0.5, 1.05 and 0.75 for sweet melon, respectively. However, the crop growth parameters should be calibrated since different areas have various different soil and climate conditions. The *LAI*, *TWU* and yield of T2 and T1 treatments in 2009 and 2008 were used to calibrate and validate the crop growth parameters, respectively. The criteria of good calibration and validation of the crop growth component were that the *RMSE* values of the simulated *LAI*, and the discrepancy between the simulated and observed yield were both lower than the standard deviation of the measurement values.

### 2.5. Scenario analysis

After calibration and validation, the coupled model was used to predict melon yield and water consumption under different irrigation scenarios and search the appropriate irrigation management practices. As shown in Table 2, there is no irrigation during blooming to fruit setting stage for T1 in 2008. Therefore, a total of 18 scenarios, i.e. 70% to 150% with an interval of 10% of the present irrigation amount of T1 during the whole growth period and fruit swelling stage were set to assess the impact of irrigation amount on yield and *WP* in 2008, respectively. In 2009, a total of 27 scenarios, i.e. 70% to 150% with an interval of 10% of the present irrigation amount of T2 during the whole growth period, blooming to fruit setting stage and fruit swelling stage were set to assess the impact of irrigation amount on yield and *WP*, respectively. Calibrated parameter values were applied in all scenarios. Yield and *WP* were used to evaluate appropriate irrigation management practices among the different irrigation scenarios. Water productivity was described as follows (Pereira et al. (2012)):

$$WP = \frac{YLD}{TWU}, \tag{21}$$

where *WP* is the water productivity ($kg\,ha^{-1}\,mm^{-1}$), *TWU* is the total water use (mm), which can be calculated as (Pereira et al. (2012))

$$TWU = P + CR + \Delta SW + I \tag{22}$$

where *P* is the seasonal amount of rainfall (mm), *CR* is the amount of water obtained from capillary rise (mm). In this study, *CR* is assumed to be 0 ascribed to the deep groundwater table. $\Delta SW$ is the difference in soil water storage between planting and harvesting (mm), and *I* is the seasonal irrigation amount (mm).

## 3. Results

### 3.1. Parameter sensitivity

It can be found that the crop growth parameters are more sensitive than the VGM model parameters with respect to the yield. As

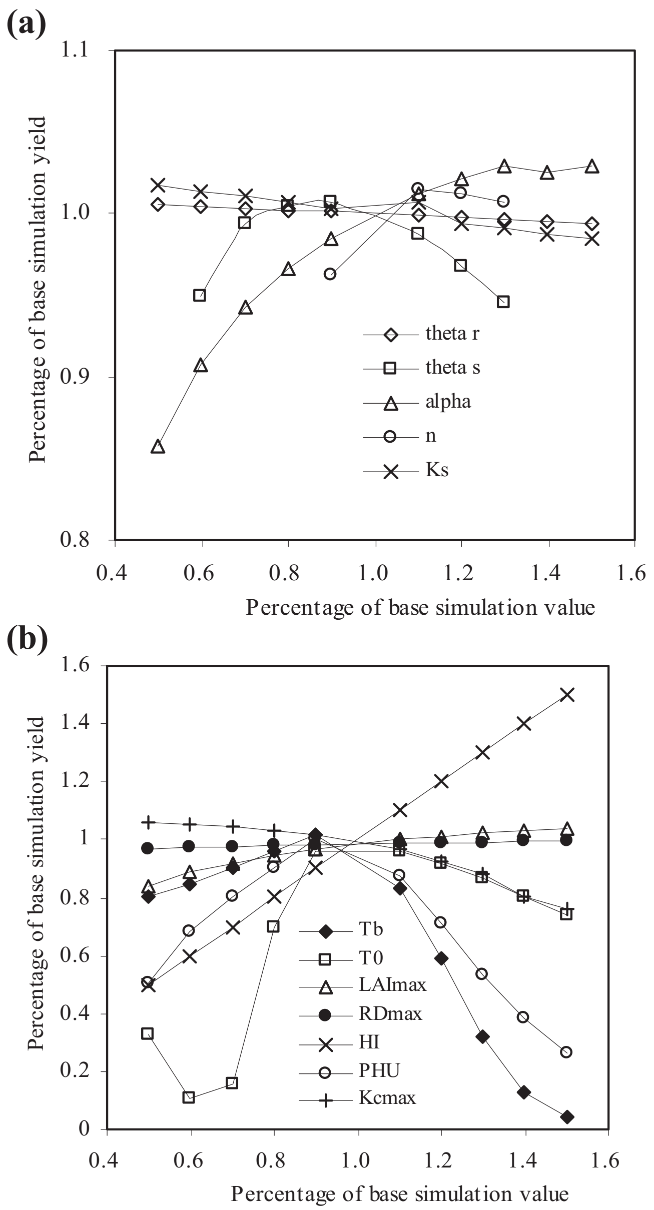


**Fig. 4.** Sensitivity analysis of the parameters with respect to yield.

shown in Fig. 4a, the most sensitive VGM model parameters with respect to yield are $\alpha$ and $n$. There is no significant effect of the parameters $\theta_r$ *and* $K_s$ on the melon yield. The sensitivity of the crop growth model parameters with respect to the yield is presented in Fig. 4b. It indicated that the optimal $T_0$, base temperatures $T_b$ and required cumulative heat unit for crop maturity *PHU* are the most sensitive parameters with respect to the yield. It can be ascribed to that the crop phonological development based on daily accumulated heat unit in the EPIC crop growth model. The yield increases as the harvest index *HI* increases. Low sensitivity of $LAI_{max}$ and $RD_{max}$ and $K_{c,max}$ is found in Fig. 4b. The relatively low sensitivity of $LAI_{max}$, $K_{c,max}$ and $RD_{max}$ to yield may be attributed to the relatively high water content in the root zone for the treatment T2 with a lower limit of soil water for irrigation of 65% FC during blooming to swelling stages. In addition, the yield decreases whenever the parameters $T_0$, $T_b$ and *PHU* increase or decrease. It indicated that the available $T_0$, $T_b$ and *PHU* are very important to the yield for the crop growth modeling.

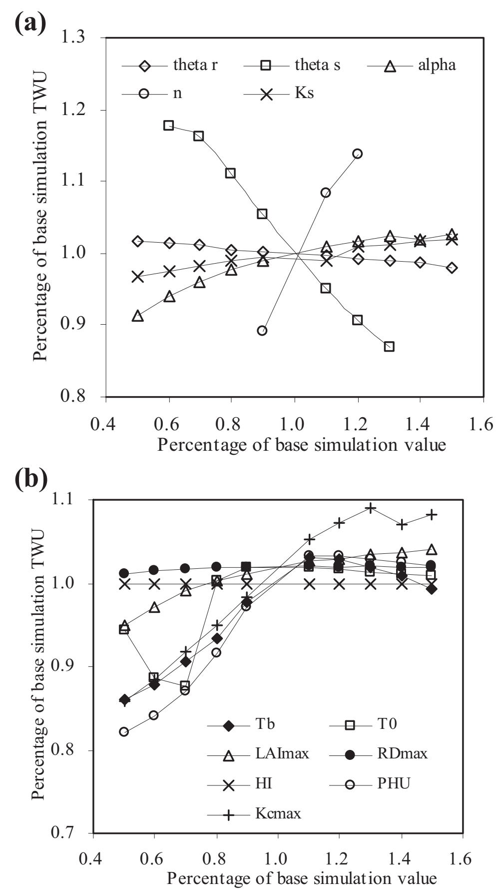


**Fig. 5.** Sensitivity analysis of the parameters with respect to total water use (*TWU*).

With respect to *TWU*, the most sensitive VGM model parameters are $\theta_r$ and $n$ (Fig. 5a). The parameter $\alpha$ is more sensitive than $\theta_r$ and $K_s$. As shown in Fig. 5b, the most sensitive crop growth model parameter is $K_{c,max}$ due to that crop transpiration is controlled by $K_{c,max}$. The parameters $T_0$, $T_b$ and *PHU* are more sensitive than $LAI_{max}$. This is ascribed to that the parameters associated to the temperature have effect on the variation of *LAI* which control the soil evaporation and crop transpiration.

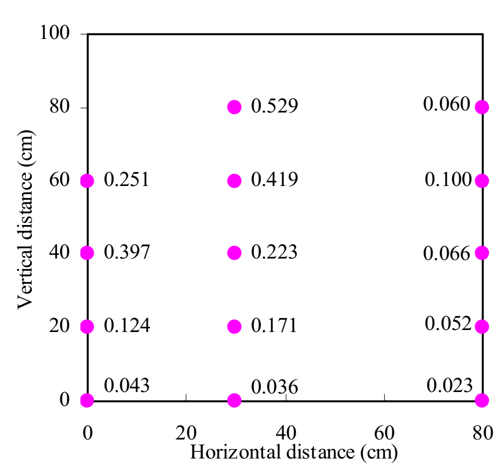


**Fig. 6.** Observed root length density in the simulating domain on July 22 (DAE 67).

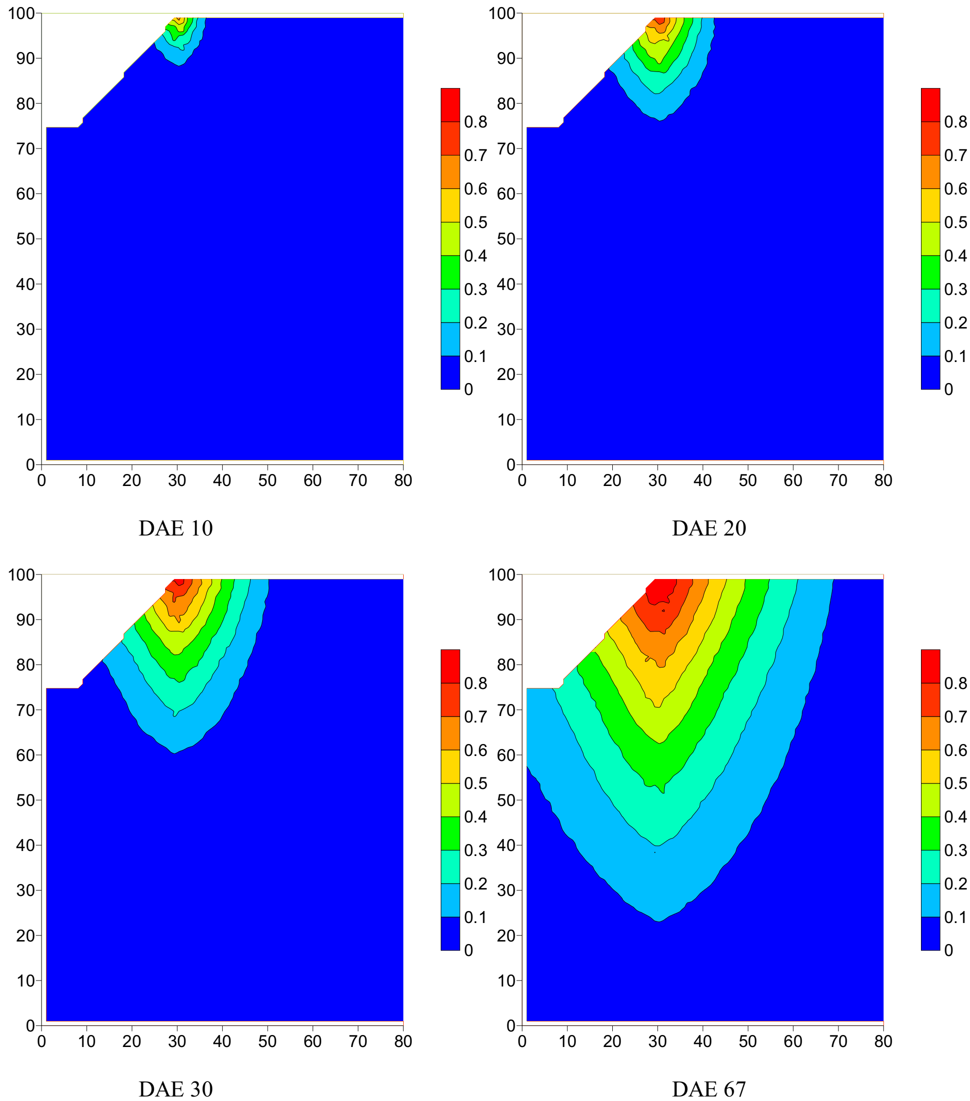


**Fig. 7.** Root distributions obtained by the coupled model at different times.

## 3.2. Calibration process

### 3.2.1. Root water uptake

We applied the GA optimization in MATLAB to get 1000 series values of the parameters. Then the parameters with the smallest values of the objective function $OF(\mathbf{s})$ were chosen as the final values of root water uptake parameters. The best estimated parameters are presented in Table 3.

As shown in Fig. 6, the root length density in upper soil layers was higher than that in lower soil layers. It can be found that the main root is located in the top 0–60 cm of soil layer and the maximum rooting length in horizontal direction is about 50 cm. In addition, the measured root length density near the furrow was higher than that in the domain of middle ridge. It may be due to the hydrotropism of melon root. With the optimized root water uptake parameters, the root water uptake distribution obtained by the coupled model is presented in Fig. 7. As shown in Fig. 7, the root water uptake distribution in the domain of the furrow bed and side was about three times higher than that in the domain of ridge and changed with time. The root water uptake distribution changed with time in the horizontal and vertical directions. However, the root depth increased with time from DAE 1 to DAE 49, and then remained at a constant value of 100 cm after DAE 49 (Fig. 8).

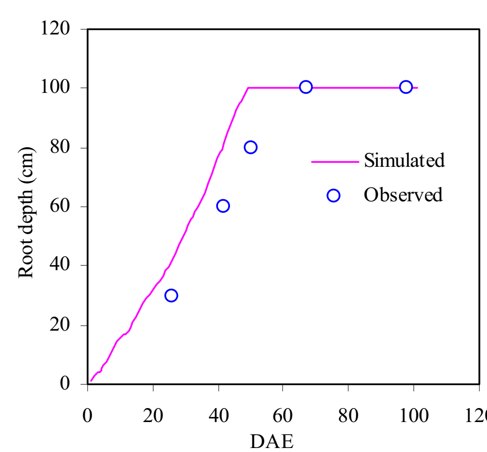


**Fig. 8.** Comparison of the observed and the simulated root depth by the coupled model.

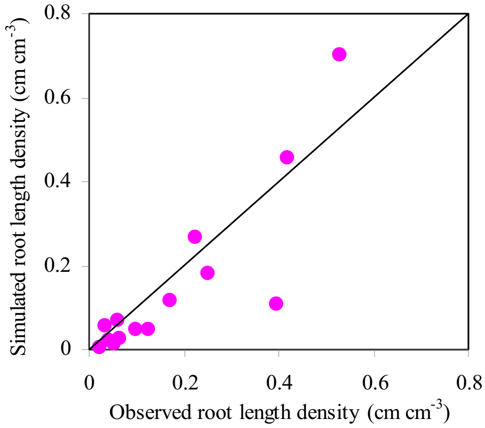


**Fig. 9.** Comparison of the observed and the simulated root length density on DAE 67.

Therefore, there is no change of the root distribution from DAE 49 to the end of the growth period (DAE 101). In addition, a relatively good agreement was found between the observed and simulated root length density on DAE 67 (Fig. 9).

### 3.2.2. Soil water content

As shown in Fig. 10, a relatively good agreement was found between measured and simulated soil water contents by the coupled model. It was found that the soil moisture in the upper soil profile changed with time more drastically than that of the deeper profile. The comparison of the observed soil water contents with the simulated values for the coupled model is shown in Fig. 10. The coupled model produced good agreement with the measured soil water contents. In addition, statistical tests were carried out to investigate the performance of the coupled model. The values of *MAE*, *RMSE* and *NSE* for soil water contents are presented in Table 4. As shown in Table 4, the *MAE* values for the coupled model were in the range of 0.012 to 0.023 $cm^3\ cm^{-3}$ for the furrow side and 0.016 to 0.028 $cm^3\ cm^{-3}$ for the middle ridge. The *RMSE* values for the coupled model were in the range of 0.015 to 0.030 $cm^3\ cm^{-3}$ and of 0.020 to 0.035 $cm^3\ cm^{-3}$ for the furrow side and middle ridge, respectively. The *NSE* values for the coupled model were in the range of 0.15 to 0.886 for the furrow side, and 0.042 to 0.769 for the middle ridge. These results indicated that the calibrated coupled model performed well in predicting the soil water content in the root zone. The calibrated soil hydraulic parameters are presented in Table 5.

### 3.2.3. LAI and yield

As shown in Fig. 11, a relatively good agreement was found between the measured and the predicted *LAI* values of the coupled model versus time. It was observed that the *RMSE* value was 0.162, whereas some of the standard deviation of the observed data was greater than 1.

In additional, the yield and *TWU* were used to evaluate the model performance. As shown in Table 6, the simulated yield was 1.73 t $ha^{-1}$ greater than the observed values. However, the standard deviation of the observed yield was 2.35 t $ha^{-1}$. The crop *TWU* simulated by the coupled model was only 10 mm greater than the observed value. The results indicated that a good calibration of the crop growth model was achieved. The calibrated parameters of the crop growth model are listed in Table 7.

## 3.3. Validation process

### 3.3.1. Soil water content

The simulated (coupled model) soil water contents in different soil layers of furrow side and middle ridge were compared with the measurement values from the melon field experiment. As shown in

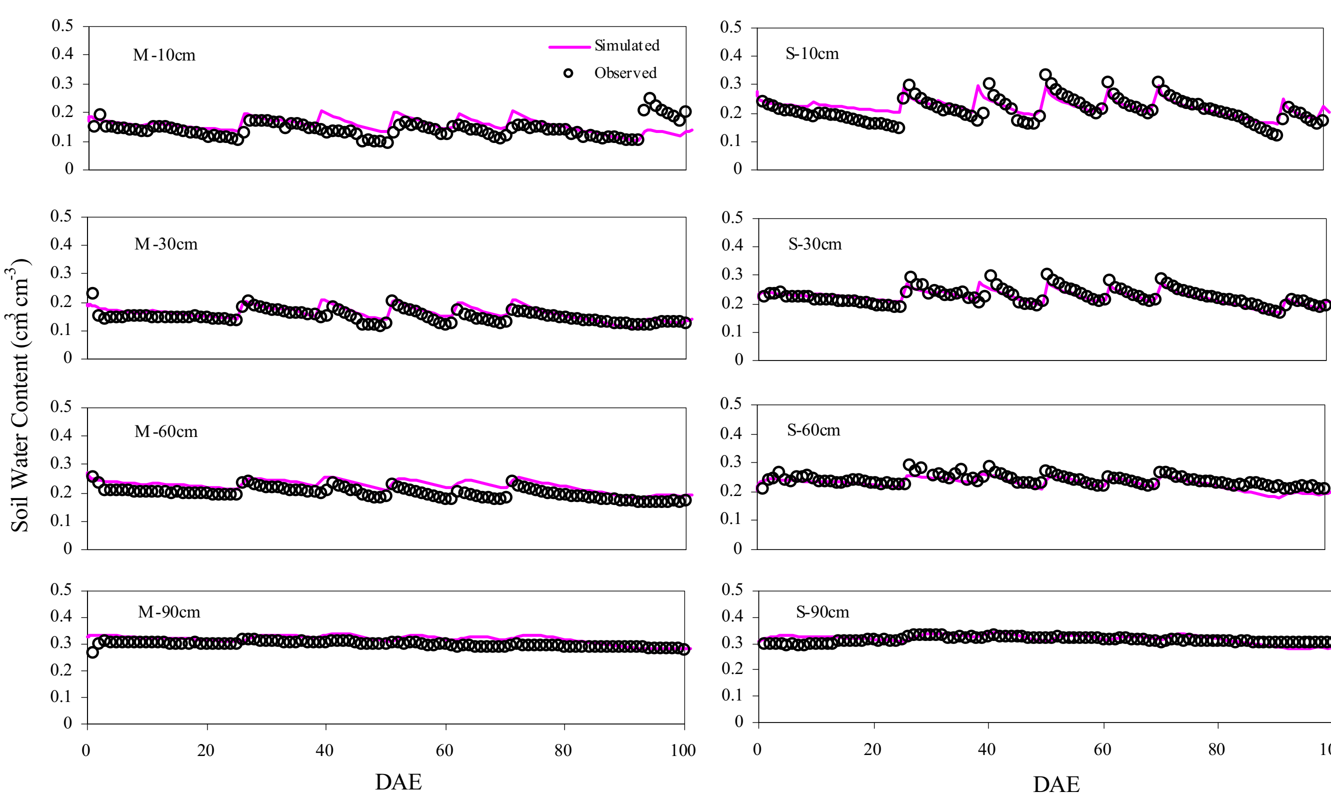


**Fig. 10.** The observed soil water content compared with the simulated by the coupled model at various soil depths of furrow side (S) and middle ridge (M) for calibration.

**Table 4**
Mean absolute error (*MAE*), root mean square error (*RMSE*) and Nash and Sutcliffe model efficiency (*NSE*) values of soil water contents at various soil depths of furrow side (S) and middle ridge (M) for calibration.

| Soil depths | M-10 cm | M-30 cm | M-60 cm | M-90 cm | S-10 cm | S-30 cm | S-60 cm | S-90 cm |
|---|---|---|---|---|---|---|---|---|
| *MAE* ($cm^3\ cm^{-3}$) | 0.028 | 0.016 | 0.028 | 0.021 | 0.023 | 0.012 | 0.014 | 0.012 |
| *RMSE* ($cm^3\ cm^{-3}$) | 0.035 | 0.020 | 0.030 | 0.024 | 0.030 | 0.016 | 0.029 | 0.015 |
| *NSE* | 0.042 | 0.348 | 0.069 | 0.769 | 0.150 | 0.886 | 0.713 | 0.819 |

**Table 5**
Calibrated soil hydraulic parameters.

| Depth (cm) | $\theta_r$ ($cm^3\ cm^{-3}$) | $\theta_s$ ($cm^3\ cm^{-3}$) | $\alpha$ (1/cm) | $n$ | $l$ | $K_s$ ($cm\ d^{-1}$) |
|---|---|---|---|---|---|---|
| 0–35 | 0.02 | 0.40 | 0.0064 | 1.870 | 0.5 | 165 |
| 35–75 | 0.02 | 0.43 | 0.0066 | 1.604 | 0.5 | 40 |
| 75–100 | 0.046 | 0.52 | 0.0085 | 1.406 | 0.5 | 25 |

*Note*: $\theta_r$ and $\theta_s$ denote the residual and saturated water contents, respectively; $\alpha$ is the inverse of the air-entry value, $n$ is a pore-size distribution index, and $l$ is a pore-connectivity parameter; $K_s$ is the saturated hydraulic conductivity.

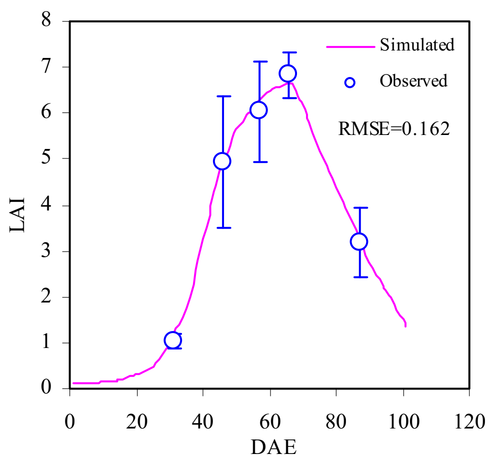


**Fig. 11.** The observed leaf area index (*LAI*) of T2 compared with the simulated by the coupled model for calibration.

Fig. 12, the coupled model produced good agreement with the measured soil water contents. The values of *MAE*, *RMSE* and *NSE* for soil water contents are presented in Table 8. However, the *MAE* values for the coupled model were in the range of 0.016 to 0.034 $cm^3\ cm^{-3}$ for the furrow side, and 0.014 to 0.035 $cm^3\ cm^{-3}$ for the middle ridge. The *RMSE* values for the coupled model were in the range of 0.019 to 0.037 $cm^3\ cm^{-3}$ and of 0.017 to 0.040 $cm^3\ cm^{-3}$ for the furrow side and middle ridge, respectively. However, the *NSE* values for the coupled model were in the range of 0.971 to 0.986 for the furrow side, and 0.971 to 0.986 for the middle ridge. The *NSE* values were greater than that obtained in calibration due to fewer data points of observed soil water content. In conclusion, the coupled model performed well in simulating soil water content in the root zone.

### 3.3.2. LAI and yield

As shown in Fig. 13, a relatively good agreement was found between measured and predicted *LAI* value versus time. It can be found that the *RMSE* value was 0.755, whereas some of the

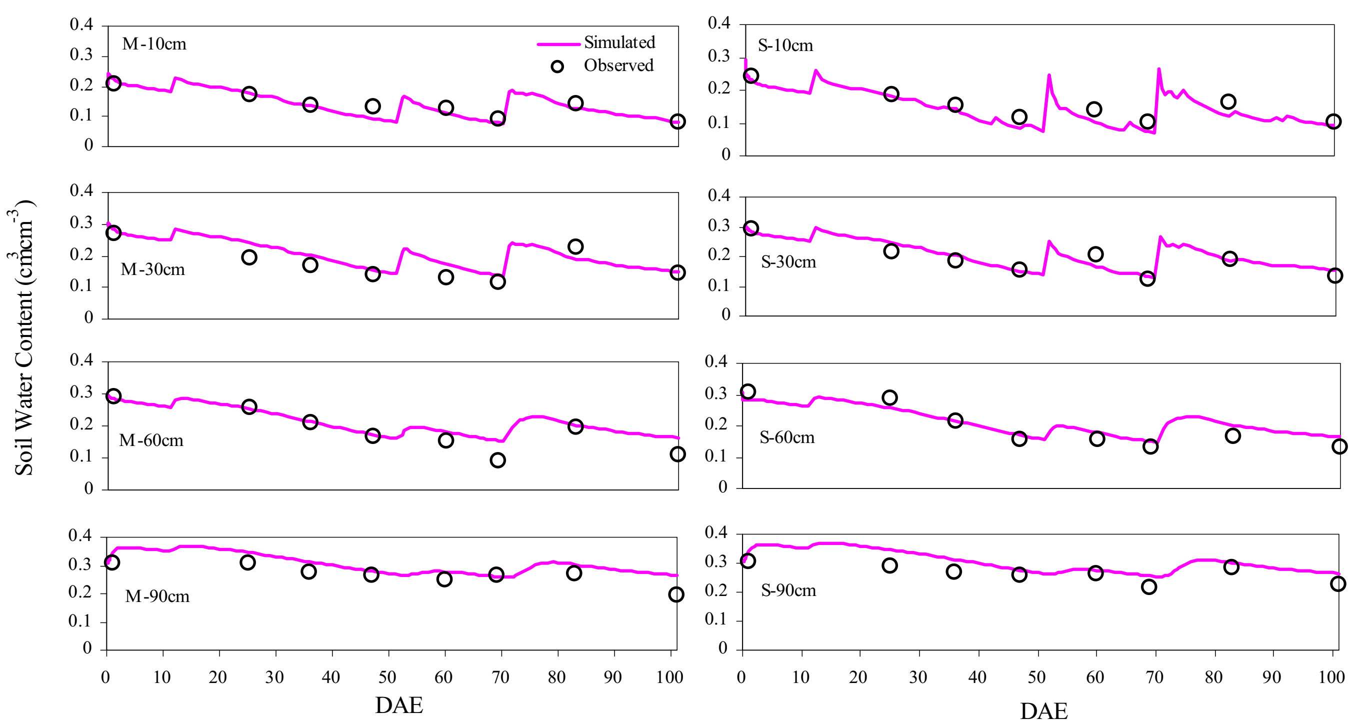


**Fig. 12.** The observed soil water contents compared with the predicted ones by the coupled model at various soil depths of furrow side (S) and middle ridge (M) for validation.

**Table 6**
Comparison between the observed and the predicted value of yield and total water use (*TWU*) for T2 by the coupled model for calibration.

| | Observed | Coupled model |
|---|---|---|
| Yield ($t\,ha^{-1}$) | 43.50 ± 2.35 | 45.23 |
| *TWU* (mm) | 325 | 335 |

**Table 7**
The parameters of crop growth model.

| Parameters | Default value | Adjusted |
|---|---|---|
| Minimum temperature for plant growth, $T_b$ (°C) | 16 | 10 |
| Optimal temperature for plant growth, $T_0$ (°C) | 32 | 22 |
| Maximum leaf area index, $LAI_{max}$ | 3 | 7 |
| Fraction of growing season controlled by cumulative temperature when leaf area index (*LAI*) starts declining, $HUI_0$ | 0.6 | 0.6 |
| Leaf area index decline rate, $\beta$ | 1 | 1 |
| Maximum root depth, $RD_{max}$ (cm) | 130 | 100 |
| Harvest index, *HI* | 0.5 | 0.4 |
| Minimum harvest index allowed for plant under the drought conditions, $H_{min}$ | 0.25 | 0.25 |
| Required cumulative heat unit for crop maturity, *PHU* | 2000 | 1100 |
| Maximum possible value of crop coefficient, $K_{c,max}$ | 1.05 | 1.2 |

*Note*: Adjusted means the values were calibrated according to the values published or suggested in the literature.

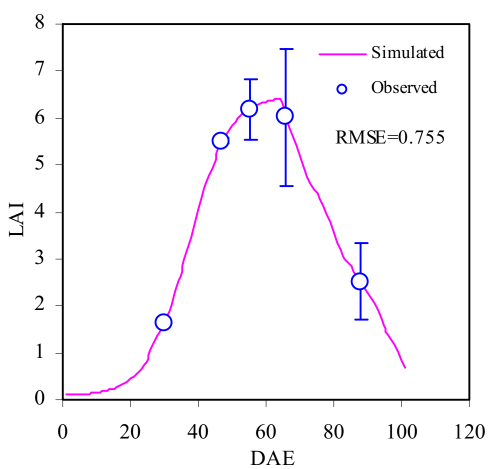


**Fig. 13.** The observed leaf area index (*LAI*) of T1 compared with the simulated by the coupled model for validation.

standard deviation of the observed data was 1.5. As shown in Table 9, the yield predicted by the coupled model was 2.19 $t\,ha^{-1}$ smaller than the observed value. However, the standard deviation of the observed yield was 1.32 $t\,ha^{-1}$. *TWU* simulated by the coupled model was lower than the observed value by 8.6%. Therefore, there is no significant difference between the simulated and observed values of melon yield.

## 4. Appropriate irrigation amounts

The most appropriate irrigation management issues should satisfy both requirements of high yields and high water productivity (Zheng et al., 2012). In this regard, Fig. 14a and b shows the

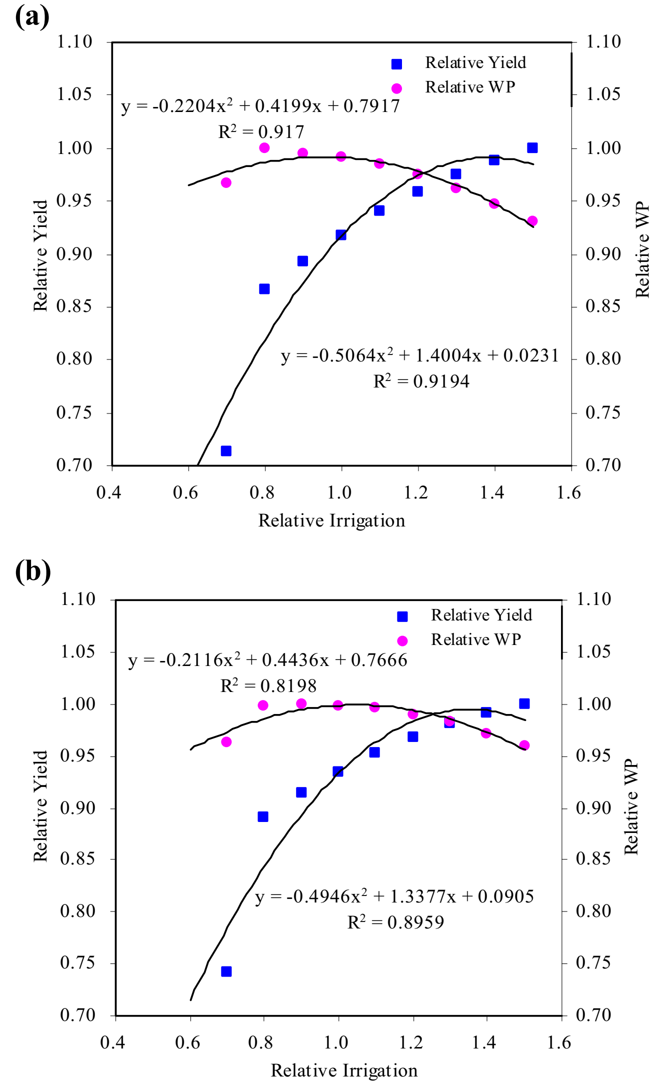


**Fig. 14.** Response of yield and water productivity (WP) to different relative irrigation during whole growth period (a) and fruit swelling stage (b) in 2008.

**Table 9**
Comparison between the observed and the predicted value of yield and total water use (*TWU*) for T1 by the coupled model for validation.

| | Observed | Coupled Model |
|---|---|---|
| Yield ($t\,ha^{-1}$) | 50.6 ± 1.32 | 48.41 |
| *TWU* (mm) | 360 | 329 |

response of relative yield and relative *WP* to the relative season irrigation for present irrigation amount of T1 during whole growth period and fruit swelling stage in 2008, respectively. In 2009, the response of relative yield and *WP* to the relative irrigation of T2 during whole growth period, blooming to fruit setting stage and fruit swelling stage are shown in Fig. 15a–c, respectively. The referred relative values were obtained for each year by dividing the

**Table 8**
Mean absolute error (*MAE*), root mean square error (*RMSE*) and Nash and Sutcliffe model efficiency (*NSE*) values of soil water contents at various soil depths of furrow side (S) and middle ridge (M) for validation.

| Soil depths | M-10 cm | M-30 cm | M-60 cm | M-90 cm | S-10 cm | S-30 cm | S-60 cm | S-90 cm |
|---|---|---|---|---|---|---|---|---|
| *MAE* ($cm^3\,cm^{-3}$) | 0.014 | 0.028 | 0.025 | 0.035 | 0.021 | 0.016 | 0.022 | 0.034 |
| *RMSE* ($cm^3\,cm^{-3}$) | 0.017 | 0.032 | 0.035 | 0.040 | 0.026 | 0.019 | 0.026 | 0.037 |
| *NSE* | 0.986 | 0.971 | 0.969 | 0.978 | 0.971 | 0.990 | 0.984 | 0.981 |

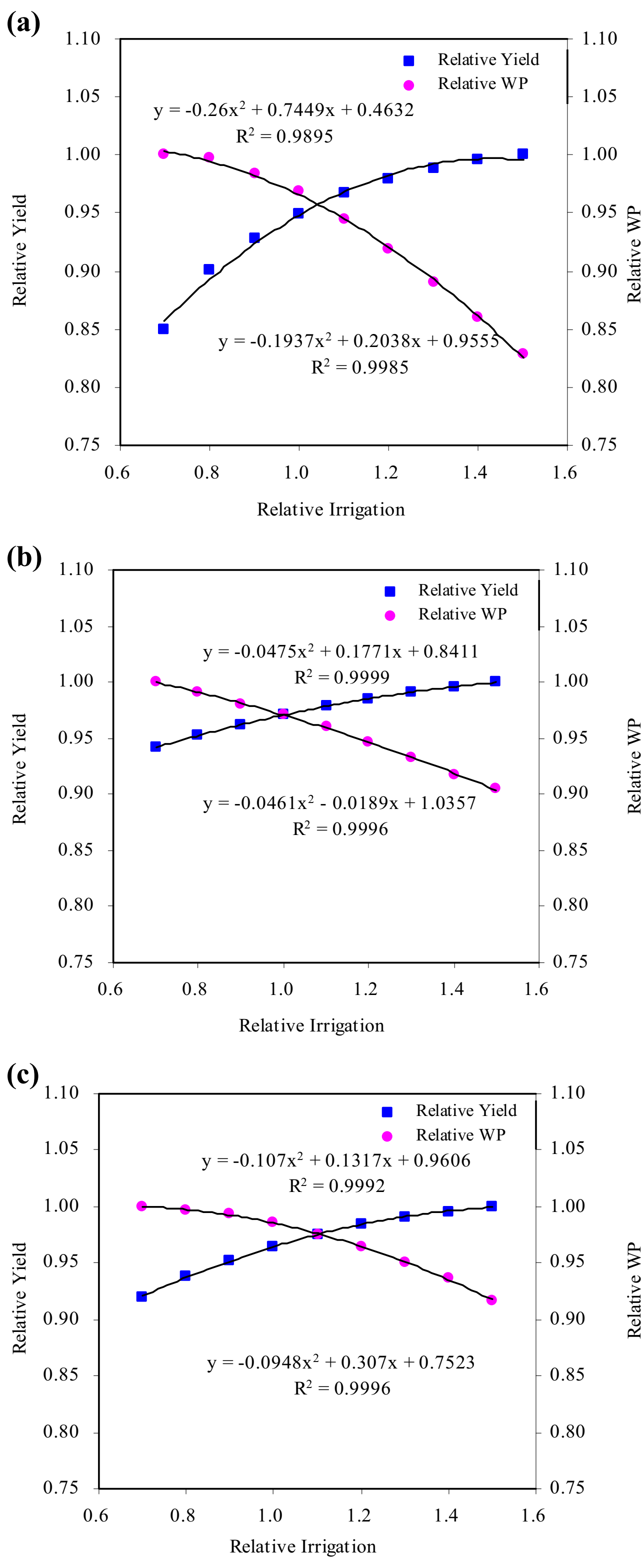


**Fig. 15.** Response of yield and water productivity (WP) to different relative irrigation during whole growth period (a), blooming and fruit setting stage (b) and fruit swelling stage (c) in 2009.

actual values by the respective maximum; hence, the values vary between 0 and 1. As shown in Fig. 14a, the relative yield increased with the increase of relative irrigation amount quadratically until a value of 1.3, while the relative WP decreased with the relative irrigation amount, and then the best result may be achieved for a relative irrigation amount of 1.2. Similar results can be obtained from Fig. 14b. In addition, Fig. 14b showed the same trend for the relative yield and *WP* versus the relative irrigation amount. It indicated that the appropriate irrigation amount was equal to 1.3 of relative irrigation amount during fruit swelling stage. Furthermore, there is no difference of the relative yield and *WP* between the two scenarios. Therefore, it can be concluded that the appropriate irrigation amount was 209 mm in 2008.

In 2009, the trend for the relative yield and *WP* versus the relative irrigation amount is the same as that of 2008. As shown in Fig. 15a, the best result may be achieved for a relative irrigation amount of 1.0 during whole growth period. However, the appropriate irrigation amount was equal to 1.0 and 1.1 of relative irrigation amount during blooming to fruit setting stage and fruit swelling stage, respectively (Fig. 15b and c). There is no difference of the relative yield between the three scenarios. Furthermore, *WP* of the scenario with relative irrigation amount of 1.0 during whole growth period was higher than those of the other two scenarios. Therefore, it can be concluded that the appropriate irrigation amount was 218 mm in 2009.

## 5. Discussions

In previous studies, change of root distribution for perennial plant cover or during short crop growth periods is usually not considered. For example, Vrugt et al. (2001) used the uniform root distribution to simulate the soil water contents under sprinkler irrigation. The results showed that the simulated and measured water contents were in excellent agreement during the 16-d period for the almond tree. However, the root distribution changes due to the root growth in the horizontal and vertical directions for annual crop or during long term. Thus, the assumption of uniform root distribution is not accurate for simulating actual crop transpiration and soil water dynamics in the root zone and to calculate the water stress constrained the crop growth. In addition, the crop parameters of the crop growth model of EPIC are mostly for the annual crop type. Therefore, the coupled model is more suitable for annual crops.

Root growth is regulated or controlled by many factors, including soil temperature, soil water content, soil strength, soil structure, soil chemical condition and soil microbiological conditions (Wang and Smith, 2004). However, root growth was not constrained in the crop growth model of EPIC. In this study, the root length in the horizontal direction was assumed to be a proportion of the rooting depth in vertical direction in the proposed root water uptake model for melon in this study. In reality, the root growth in the horizontal direction is constrained with the soil water content, soil strength and other factors. In addition, young roots can grow, proliferate, transform into mature roots and then decay. Acock and Pachepsky (1996) described root growth and proliferation as a convective-diffusive process and considered the root decay rate. However, as shown in Fig. 8, the root depth increased with time, and then remained a constant value of 100 cm in the last 50 days of the growth period. In addition, the observed root depth was lower than the simulated value during the early growth period. This may be due to that the regulate factor for the root growth was not considered in this study. If above-mentioned factors were all integrated into the proposed root distribution function, the coupled model was expected to perform better in simulating soil water dynamics under 2D domain with crop. This issue also deserves further study.

Although the coupled model was calibrated by the experimental data under furrow irrigation, it can also be used to simulate the soil water dynamics in the root zone under other irrigation conditions, for example drip irrigation. In other words, the coupled model can simulate water movement in 2D domain with crop growth. However, the compensation of root water uptake was not considered in this study due to that the root adaptability factor $\omega_c$ should be calibrated using the detail data of soil water content for the severe stress treatment. Therefore, compensated root water uptake will be involved in our follow-up investigation. In addition, it is worthy of further investigation whether the model can be used or not for simulating soil water dynamics and crop growth for those conditions with soil cracking, severe water stress condition, etc.

## 6. Conclusions

In this study, a new 2D root water uptake model was developed by integration of the Vrugt model and the root growth model. Then, a new coupled model was developed based on the CHAIN_2D and the crop growth model of EPIC. The coupled model was calibrated and validated by the observed values obtained from melon field experiment conducted by the authors. The root growth and root water uptake distribution, soil water contents, leaf area index (*LAI*), melon yield and total water use (*TWU*) were simulated by the coupled model. The simulation results of the coupled model were compared with experimental results obtained from a melon field experiment. After calibration and validation, the coupled model was used to assess the impact of irrigation amounts, i.e. 70% to 150% with the interval of 10% of the present irrigation amounts of T1 and T2 during the whole growth period, blooming to fruit setting stage and fruit swelling stage in 2008 and 2009, respectively. The relative yield and water productivity (*WP*) of the different irrigation scenarios were considered as the criteria for investigating the appropriate irrigation management practices. Several conclusions can be obtained from this research:

(1) The proposed root water uptake model can be used to better describe the interaction between crop growth and actual root water uptake more realistically.

(2) The coupled model with the proposed root water uptake model can be used to simulate dynamic root water uptake distribution, soil water content and yield under furrow irrigation for annual crop.

(3) Considering the yield and *WP*, the appropriate seasonal irrigation amount for melon obtained by using the coupled model was 209 mm in 2008 and 218 mm in 2009, respectively at the study area.

## Acknowledgments

This research was jointly supported by National Natural Science Foundation of China (51125036, 51039007), and the China-Israel Joint Research Program (CIJRP 2010006).

## References

Abbasi, F., Feyen, J., van Genuchten, M.Th., 2004. Two dimensional simulation of water flow and solute transport below furrows: model calibration and validation. J. Hydrol. 290, 63–79.

Acock, B., Pachepsky, Y.A., 1996. Convective-diffusive model of two dimensional root growth and proliferation. Plant Soil 180, 231–240.

Ajdary, K., Singh, D.K., Singh, A.K., Khanna, M., 2007. Modelling of nitrogen leaching from experimental onion field under drip fertigation. Agric. Water Manage. 89, 15–28.

Allen, R.G., Pereira, L.S., Raes, D., Smith, M., 1998. Crop evapotranspiration. In: FAO Irrigation and Drainage Paper No.56. FAO, Rome.

Crevoisier, D., Popova, Z., Mailhol, J.C., Ruelle, P., 2008. Assessment and simulation of water and nitrogen transfer under furrow irrigation. Agric. Water Manage. 95, 354–366.

de Willigen, P., Heinen, M., Mollier, A., van Noordwijk, M., 2002. Two-dimensional growth of a root system modelled as a diffusion process. I. Analytical solutions. Plant Soil 240, 225–234.

Doltra, J., Muñoz, P., 2010. Simulation of nitrogen leaching from a fertigated crop rotation in a Mediterranean climate using the EU-Rotate_N and Hydrus-2D models. Agric. Water Manage. 97, 277–285.

Feddes, R.A., Kowalik, P.J., Zaradny, H., 1978. Simulation of Field Water Use and Crop Yield. John Wiley & Sons, New York, NY.

Gao, Y., Duan, A., Qiu, X., Liu, Z., Sun, J., Zhang, J., Wang, H., 2010. Distribution of roots and root length density in a maize/soybean strip intercropping system. Agric. Water Manage. 98, 199–212.

Hanson, B.R., Šimůnek, J., Hopmans, J.W., 2006. Evaluation of urea-ammonium-nitrate fertigation with drip irrigation using numerical modeling. Agric. Water Manage. 86, 102–113.

Kang, S.Z., Cai, H.J., Chen, Y., Shen, Q.L., Kong, D.L., 1996. The water-saving approach and countermeasures for agriculture with high efficiency in the Shiyang River valley of the west of the Yellow River. Agric. Res. Arid Area 14 (1), 10–18 (in Chinese with English abstract).

Kang, S.Z., Su, X.L., Tong, L., Shi, P.Z., Yang, X.Y., ABE, Y., Du, T.S., Shen, Q.L., Zhang, J.H., 2004. The impacts of human activities on the water–land environment of the Shiyang River basin, an arid region in northwest China. Hydrol. Sci. J. 49 (3), 413–427.

Li, S., Kang, S., Li, F., Zhang, L., 2008. Evapotranspiration and crop coefficient of spring maize with plastic mulch using eddy covariance in northwest China. Agric. Water Manage. 95, 1214–1222.

Li, Y., White, R., Chen, D.L., Zhang, J.B., Li, B.G., Zhang, Y.M., Huang, Y.F., Edis, R., 2007. A spatially referenced water and nitrogen management model (WNMM) for (irrigated) intensive cropping systems in North China Plain. Ecol. Modell. 203, 395–423.

Li, Y.J., Yuan, B.Z., Bie, Z.L., Kang, Y.H., 2012. Effect of drip irrigation criteria on yield and quality of muskmelon grown in greenhouse conditions. Agric. Water Manage. 109, 30–35.

Lu, C., Yang, J., Jayawardane, N., Tan, Y., Biswas, T., 2004. Numerical modeling of nitrogen transport and transformation in sewage irrigation and treatment system. J. Hydraul. Eng. 5, 83–88 (in Chinese with English abstract).

Mailhol, J.C., Crevoisier, D., Triki, K., 2007. Impact of water application conditions on nitrogen leaching under furrow irrigation: experimental and modelling approaches. Agric. Water Manage. 87, 275–284.

Mmolawa, K., Or, D., 2003. Experimental and numerical evaluation of analytical volume balance model for soil water dynamic under drip irrigation. Soil Sci. Soc. Am. J. 67, 1657–1671.

Monteith, J.L., 1977. Climate and the efficiency of crop production in Britain. Philos. Trans. R. Soc. London, Ser. B 281, 277–294.

Mualem, Y., 1976. A new model for predicting the hydraulic conductivity of unsaturated porous media. Water Resour. Res. 12, 513–522.

Pereira, L.S., Cordery, I., Iacovides, I., 2012. Improved indicators of water use performance and productivity for sustainable water conservation and saving. Agric. Water Manage. 108, 39–41.

Sensoy, S., Ertek, A., Gedik, I., Kucukyumuk, C., 2007. Irrigation frequency and amount affect yield and quality of field-grown melon (*Cucumis melo* L.). Agric. Water Manage. 88, 269–274.

Šimůnek, J., van Genuchten, M.Th., 1994. The CHAIN_2D Code for Simulating Two-Dimensional Movement of Water, Heat, and Multiple Solutes in Variably-Saturated Porous Media. U.S. Salinity Laboratory Agricultural Research Service, U.S. Department of Agriculture, Riverside, CA.

Šimůnek, J., van Genuchten, M.Th., Šejna, M., 2008. Development and applications of the HYDRUS and STANMOD software packages, and related codes. Vadose Zone J. 7 (2), 587–600, http://dx.doi.org/10.2136/VZJ2007.0077.

Siyal, A.A., Bristow, K., Šimůnek, J., 2012. Minimizing nitrogen leaching from furrow irrigation through novel fertilizer placement and soil surface management strategies. Agric. Water Manage. 115, 242–251.

van Genuchten, M.Th., 1980. A closed-form equation for predicting the hydraulic conductivity of unsaturated soils. Soil Sci. Soc. Am. J. 44, 892–898.

Vrugt, J.A., Hopmans, J.W., Šimůnek, J., 2001. Calibration of a two-dimensional root water uptake model. Soil Sci. Soc. Am. J. 65, 1027–1037.

Wang, E., Smith, C.J., 2004. Modelling the growth and water uptake function of plant root systems: a review. Aust. J. Agric. Res. 55, 501–523.

Williams, J.R., Jones, C.A., Kiniry, J.R., Spanel, D.A., 1989. The EPIC crop growth model. Trans. ASAE 32 (2), 497–511.

Williams, J.R., Wang, E., Meinardus, A., Harman, W.L., Simers, M., Atwood, J.D., 2006. EPIC Users Guide v. 0509, ⟨http://epicapex.brc.tamus.edu/media/23015/epic0509usermanualupdated.pdf⟩.

Willmott, C.J., 1982. Some comments on the evaluation of model performance. Bull. Am. Meteorol. Soc. 63 (11), 1309–1313.

Wöhling, Th., Schmitz, G.H., 2007. Physically based coupled model for simulating 1D surface-2D subsurface flow and plant water uptake in irrigation furrow. I: Model development. J. Irrig. Drain. Eng. 133 (6), 538–547.

Wöhling, Th., Mailhol, J.C., 2007. Physically based coupled model for simulating 1D surface-2D subsurface flow and plant water uptake in irrigation furrow. II: Model test and evaluation. J. Irrig. Drain. Eng. 133 (6), 548–558.

Zheng, J., Huang, G., Wang, J., Huang, Q., Pereira, L.S., Xu, X., Liu, H., 2012. Effects of water deficits on growth, yield and water productivity of drip-irrigated onion (*Allium cepa* L.) in an arid region of Northwest China. Irrig. Sci., http://dx.doi.org/10.1007/s00271-012-0378-5.

Zhou, Q., Kang, S., Zhang, L., Li, F., 2007. Comparison of APRI and Hydrus-2D models to simulate water dynamics in a vineyard under alternate partial root zone drip irrigation. Plant Soil 291, 211–223.